Role of Proximal His93 in Nitric Oxide Binding to Metmyoglobin. Application of Continuum Solvation in Monte Carlo Protein Simulations

György M. Keserű*,‡ and Dóra K. Menyhárd§

Department of Chemical Information Technology, Technical University of Budapest, Szt. Gellért tér 4, H-1111 Budapest, Hungary, and Department of Theoretical Chemistry, Eötvös University, Pázmány Péter sétány 2, H-1117 Budapest, Hungary

Received July 7, 1998; Revised Manuscript Received January 28, 1999

ABSTRACT: Monte Carlo protein simulations with continuum solvation were used to explore the conformational mobility of NO within the active site of metmyoglobin. To the best of our knowledge this is the first application of a continuum solvation model for exploring protein binding sites. The usefulness of the Monte Carlo conformational analysis was demonstrated in comparative molecular dynamics simulations. Analysis of conformer populations revealed that Monte Carlo conformational analysis is more effective in mapping the relevant region of the potential surface. Distribution of low-energy conformers obtained for the metmyoglobin−NO complex was found to depend on the orientation of proximal His93. Different charge distributions corresponding to the two experimentally verified possible torsions of this proximal residue result in strong binding of NO or its release to a nearby hydrophobic trap. Conformer populations obtained by Monte Carlo conformational analysis were grouped into three main families: one, with the NO directly bound to the iron, appears when the CA−CB−CG−CD2 torsion of His93 is at its ligand binding value (−113°); and two conformers exist where NO is trapped in a nearby hydrophobic pocket, the same cavity that was determined to be the geminate trap of CO in ferrous Mb as a result of the torsional flip of His93 to its ligand releasing state (−125°). Based on this analysis, we suggest that the electrostatic rearrangement coupled to the conformational fluctuation of the proximal His leads to the geminate trapping of the ligand. Conformational rearrangement of the proximal side would provide the possibility of rebinding of the ligand to Fe.

Molecular dynamics (MD)[1] simulations are widely used for the evaluation of energetically favored binding conformations of protein−substrate complexes. Until recently MD was also the preferred methodology used for the calculation of binding free energies for enzyme−substrate complexes on the basis of the free energy perturbation (FEP) theory (*1*). It is well-known, however, that a protein becomes trapped in a certain region of conformational space and may never escape—no matter how long the MD simulation runs (*2, 3*). Moreover conformations separated by relatively high energy barriers are usually inefficiently sampled in MD. These sampling problems can easily be overridden using MC-based conformational searching algorithms. In addition to this advantage, the statistical treatment applied in MC does not require any extra coupling algorithms which are used in MD simulations (*4*). Furthermore, thermal artifacts usually associated with the MD treatment of nonbonded interactions can also be avoided using MC methods. In contrast to conventional Metropolis Monte Carlo (MMC) simulations, we performed a Monte Carlo based conformational analysis (MCMM). The effectiveness of the this approach for the calculation of protein−substrate complexes was demonstrated in our previous comparative MC/MD study (*5*) on cytochrome P450 and was recently extended to cytochrome P450 inhibitors evaluating low-energy binding modes to rationalize their mode of action (*6*). The Metropolis Monte Carlo methodology has also shown considerable success in free energy calculations (*7, 8*) and was recently applied to protein−substrate complexes too by Jorgensen et al. (*9*). The effectiveness of this approach was also demonstrated in a comparative MC/MD study for liquid hexane by Jorgensen et al. (*10*). Excellent agreement obtained between calculated and experimental relative binding free energies for a number of trypsin inhibitors (*11*) gave further support to the usefulness of the MC approach. It should be noted, however, that the Metropolis MC applied in these studies is very different from the MC conformational analysis applied by our group. Although this MMC study was performed using a highly sophisticated protocol, external degrees of freedom of substrates were not considered in aqueous phase calculations. This limitation possibly originated from the increased computational cost associated with solvating the system using a TIP4P explicit water model (*12*) and also with hundreds of thousands of MC steps required for adequate sampling. Although the application of molecular solvent models such as the TIP4P represents a convenient way for consideration

‡ Technical University of Budapest.

§ Eötvös University.

[1] Abbreviations: FEP, free energy perturbation; Hb, hemoglobin; Mb, myoglobin; MC, Monte Carlo; MCMM, Monte Carlo multiple minimum search; MD, molecular dynamics simulation; MMC, Metropolis Monte Carlo simulation; MOLS, variable molecule selection; PB, Poisson−Boltzmann equation; SUMM, systematic unbounded multiple minimum search; TNCG, turncated Newton conjugate gradient optimization.

10.1021/bi981611v CCC: $18.00
Published on Web 04/29/1999

of the liquid medium, the large number of solvent molecules and solvated states impose major limitations. Problems arising from explicit solvent models prompted us to use the GB/SA model (*13*) for protein optimizations (*6*). Here we report a study using the GB/SA continuum solvation model in docking calculations using Monte Carlo conformational analysis instead of Metropolis MC simulations which allows us to perform MC docking considering solvation effects and external degrees of freedom of the ligand as well. Complexation of NO to metmyoglobin was chosen to test our methodology. In addition to the fact that this system is currently the focus of general interest, the small molecular volume of NO relative to the binding pocket represents an ideal test case to explore the unusually large degrees of translational and rotational freedom of the ligand.

NO is a unique ligand of the globins [hemoglobin (Hb), myoglobin (Mb)] in the sense that it binds to the iron regardless of its oxidation state, and is even responsible for the interconversion of its different redox states. In the presence of oxygen, NO readily oxidizes Hb/MbFe(II) to their respective met state, Hb/MbFe(III) (*14*). In the absence of oxygen, it can do the reverse: it reduces Hb/MbFe(III) to their active Hb/MbFe(II) form (*15, 16*). NO can also protect from possible oxidative damages caused by the formation of Hb/MbFe(IV)═O species by reducing this form to Hb/MbFe(III) (*17*).

The physiological functions of NO are numerous. NO is a key intercellular signal and defensive cytotoxin in the nervous, muscular, cardiovascular, and immune systems (*18*). NO has been recognized as the endothelial-derived relaxing factor (*19, 20*); its vasodilatory and antithrombotic activity (*21*) and its effect on platelet aggregation and macrophage function have also been demonstrated (*14*). NO-bound HbFe(II) have been detected in the venous blood system of animals exposed to oxidative stress (*22*) or hyperthermia.

The MbFe(III)−NO complex studied in this work is a spectroscopically stable species, with an equilibrium constant of $1.41 \times 10^4\ M^{-1}$, whose reduction to MbFe(II)−NO is a slow process (*16*). The dynamics of this complex have been shown by various experimental methods to be similar to those of its isoelectronic pair, MbFe(II)−CO (*15, 23*), where the release of CO from the Fe is thought to proceed through a four-step pathway (*24*):

$$\underset{\text{bound}}{\text{MbCO}} \rightarrow \underset{\text{distal pocket}}{\text{Mb:CO}} \rightarrow \underset{\text{protein matrix}}{\text{Mb::CO}} \rightarrow \underset{\text{in solvent}}{\text{Mb} + \text{CO}}$$

with the CO first geminately trapped in a nearby docking site in two opposing orientations as determined by a laser flash photolysis study (*25*).

Ligand motion within the active site pocket of Mb and geminately trapped conformations has been studied on photodissociated complexes using both experimental and theoretical methods (*25*−*30*). However, since laser flash photolysis can hardly be designated as a physiological process, it would be of primary interest to see whether a specific conformational change of the protein could be identified which would induce a similar ligand response. The nature and conformation of the two closest reaching amino acids—the distal His64 and proximal His93 in the wild-type protein—have been shown to have the most dominant effect on ligand binding (*31*−*34*). We have recently shown (*35*) that the flip of the proximal His93 (that anchors the heme group) along its CA−CB−CG−CD2 torsion angle (Figure 1) causes changes in the bonding system and charge distribution at the active site of the MbFe(III)−NO complex and provides energetic stabilization of the NO-free heme. In this present work, we probed whether the resultant different electrostatic environment can, in itself, bring about the dissociation of NO from the iron and its geminate trapping in the protein interior. MCMM methodology applied with continuum solvation allowed us to explore the conformational space of NO both in the iron-bound and in the geminately captured state.

MATERIALS AND METHODS

Docking Methodology. The high-resolution crystal structure of metmyoglobin was obtained from the Brookhaven Protein Databank (code 1ymb) (*36*). A binding site model was defined as an approximately 15 Å sphere around the central heme. This model is composed of 89 amino acids and the Fe(III) heme unit including the NO substrate. NO was placed 1.96 Å from the iron in a bent conformation, based on small molecular crystallographic results for a model heme compound (*37*) and the structure of the HbFe(III)−NO (*38*) complex. All calculations were performed using the all-atom implementation of the AMBER* force field (*39*) available in the MacroModel 6.0 package (*40*). This force field is identical to the original AMBER with the exception of backbone parameters. Electrostatic treatment of the system involved a distance-dependent dielectric constant ($\epsilon = 4$) (*41*) at this stage of calculations. We used heme parameters (available from http://munim.ucsf.edu/amber/ff94/contrib/heme) generated by David Case at Scripps and modified by Chris Bayly at Merck Research Laboratories. Heme atoms and NO carried their ab initio derived charges (*35*); AMBER all-atom charges were used for amino acid residues. Since crystal structures even refined in high resolution might contain several unfavorable interactions, the crystal structure was first relaxed using 20 steps of steepest descent minimization (*42*). Relaxation was followed by conjugate gradient optimization utilizing the Polaak−Ribiere algorithm and the convergence criteria of 0.002 kcal/(mol·Å) to obtain the starting geometry for further simulations.

The 89 amino acids of the binding site model were not contiguous in the protein, and therefore all the backbone atoms had to be constrained (constrained-shell system). 100 kJ/Å^2 constraints were introduced by a harmonic restoring potential for the porphyrin unit and for main chain atoms outside a 10 Å sphere around the central iron atom. All other backbone atoms were constrained by a 20 kJ/Å^2 tethering function. Partial restraint on active site amino acids was introduced because ligand diffusion within the cavity is a much faster motion than the responding protein conformational rearrangement. However, to verify the constraint substructure shell system applied, calculations were repeated without constraints on active site residues. Cutoff distances were extended to 8 Å for van der Waals interactions, and infinite cutoff distances were used for charge−charge interactions considering the long-range electrostatic interactions in the protein. The electrostatic effects of the protein environment associated with different orientations of the proximal His93 were calculated using charge distributions

obtained for two different values of its CA−CB−CG−CD2 torsion.

Solvation effects were considered using the GB/SA continuum solvation model. A detailed description of this model is given in the Appendix. It should be noted that the analytical implementation of the GB model in MacroModel 6.0 is based on stretch, bend, and nonbonded interactions. This also means that long-range electrostatic polarization is taken into full consideration by the application of infinite electrostatic cutoffs. The continuum model was used due to the problems associated with the explicit solvent systems for screening solvation effects. The multiple minimum problem arising from the huge number of local minima for the solvent represents the most important factor against the usage of explicit solvation in protein optimization and conformational analysis of enzyme−substrate complexes. Calculations using explicit solvents generally require several orders of magnitude more CPU time than the corresponding gas-phase calculations with the solute molecule alone. Since virtually all biological applications involve macromolecules, cutback on CPU time is of prime importance. Continuum models treating the solvent as a continuous medium exhibiting the average properties of real solvents represent a viable alternative of the explicit model. The accuracy of the continuum model applied, however, is of crucial importance. In a recent study Friesner et al. (*43*) compared solvation free energies obtained from a number of approximate continuum models including the GB/SA solvation model (*13*) with an accurate solution of the Poisson−Boltzmann equation (PB) (*44*) for peptides. This comparison showed the predictive power of the GB/SA model to be the best. Solvation free energies were in high correlation with the results obtained by the most sophisticated PB model. This success achieved by GB/SA for single-point calculation of solvation effects in peptides and proteins reassured us in using this model for protein simulations as well. Furthermore, it should be noted that there is no compelling evidence that computationally expensive simulations involving explicit solvent molecules are better than continuum solvation models (*45*). This was demonstrated by comparison of conformational preferences of the alanine dipeptide obtained with the GB continuum model and explicit solvation (*46*). Additional calculations with a finite difference PB equation revealed that solvation energies can be accurately calculated using GB continuum solvation. The effectiveness of the GB approach was also demonstrated by single-point calculation of solvation effects in proteins (*47*). In conclusion, continuum models avoid these difficulties and therefore are ideal for the simulation of complex systems. To the best of our knowledge, the present work is the first application of a continuum model for the conformational analysis of a ligand within an enzyme active site.

Sampling efficiency of computer simulations also has a characteristic effect on the evaluation of conformer populations. It should be noted that the atomic or internal coordinate constraints used for efficient sampling (e.g., SHAKE) can be more readily introduced to MC than to MD. Systems that have multiple conformations separated by high-energy barriers represent a special case for adequate sampling. This is the typical situation in docking a small molecular substrate to a macromolecular binding site, when direct interconversion between low-energy binding modes is limited. Exploration of the total conformational space of the protein−substrate complex requires the adequate sampling of all significantly populated conformers (global sampling) and their local conformational space as well (local sampling). Due to the low probability associated with barrier crossings, conformers separated by high barriers are usually sampled inefficiently in MD. This results in sampling that is limited to the local space of some possible conformations which might even be restricted to the starting conformation. This can be expected when conformers are separated by extremely high barriers. However, torsional barriers even no higher than 3−5 kcal/mol can cause sampling problems in MD simulations (*48*−*50*). On the other hand, MC methodology has a unique capability to interconvert conformers along high-energy conformational pathways. This ultimate feature of MC was substantiated in a number of highly efficient MC-based conformational search methodologies such as the Monte Carlo multiple minimum (MCMM) (*51*) applied here, the systematic unbounded multiple minimum (SUMM) (*52*), and the low-mode (LMOD) (*53*) conformational searches. These algorithms were implemented to the MacroModel package and extensively used for the conformational analysis of organic host−guest complexes (see, e.g., ref *54*).

The differences between the most widely used MMC method and the MCMM search used by us are characteristic. The Metropolis Monte Carlo algorithm generates a large number of trial stuctures rapidly whose acceptance is subject to a simple probabilistic rule. A minimum energy conformation, *X*, is subjected to random variation of coordinates (e.g., Cartiesian or internal coordinates), and the energy of the resulting *Y* structure is evaluated. If $E_Y < E_X$, structure *Y* is accepted as a starting structure of energy minimization (or it can be simply accepted without it) to produce a new conformation. If $E_Y > E_X$, structure *Y* is accepted only if a random number drawn from the uniform distribution in the 0,1 interval is less than the Boltzmann population calculated by the formula:

$$r = e^{-[(E_Y - E_X)/RT]}$$

The Boltzmann probability applied in the Metropolis Monte Carlo method assumes that the system is thermally equilibrated, and it can be shown that the Metropolis algorithm, in the limit, explores different regions of the conformational space according to their Boltzmann probability. In conclusion, low-energy regions are explored more frequently than high-energy regions; however, this is only true after a huge number of MC steps.

The usage-directed Monte Carlo conformational search algorithm, however, has proven to be more efficient in focusing the search on the low-energy conformers than Metropolis MC and therefore requires much fewer steps. This search is based on the fact that random trial structures generated from low-energy conformers usually afford low-energy conformations after energy minimization, while minimizations of conformations generated from high-energy structures lead to new high-energy conformers. Starting structures for this algorithm are chosen from only the low-energy region, random variations to selected internal coordinates are applied, the structure is minimized, and the result is compared with minima found during previous search steps. In the framework of the Monte Carlo conformational search,

this sequence is termed a Monte Carlo step and the entire procedure a Monte Carlo multiple minimum (MCMM) search. It should be noted that the conventional MC step does not involve energy minimization as it is usual in MD as well. The MCSM (Monte Carlo single minimum) search developed by Scheraga (*55*) applies energy minimization for structures generated by MC, but this search could not be restricted to chemically relevant low-energy conformations. The MCMM algorithm, however, chooses a range of low-energy starting geometries (in our case, this range was set to 50 kJ/mol relative to the actual global minimum) and uses such structures uniformly. The method keeps track of the number of times a particular low energy conformation has been found and always uses the one used the least frequently to generate the next trial structure. Furthermore, it was demonstrated that instead of always varying the same number of internal coordinates at each MC step, it is better to choose a random number of such coordinates to be varied from between 1 and some maximum number of them. Selecting starting geometries from the previously found low-energy conformations and using such structures an equal number of times in combination with the random variation of internal coordinates to be changed in a MC step make this methodology particularly efficient. One of the main reasons why MCMM is so efficient is that MCMM is not subject to energy barriers. The random perturbation applied is a geometrical operation; it is not affected by the shape of the potential energy surface. The subsequent energy minimization—TNCG with sophisticated line search—can also easily pass high-energy barriers and kind of break its way through rough terrain downhill toward some low-energy minimum. Neither Metropois MC nor MD has this advantage.

The MCMM search, therefore, takes advantage both of energetically favorable torsional variations and of more random jumps into remote regions of the conformational space. Thus, MCMM employs a combination of torsionally local search steps and global conformational changes which allow exploration of virtually all low-energy conformations at the potential energy surface.

In summary, Metropolis MC (MMC) is a simulation technique driven by the Metropolis algorithm to surmount energy barriers, whereas MC conformational analysis is a stochastic method to explore conformational space which is not affected by energy barriers at all. The use of rotamer libraries can in principle alleviate the low acceptance rate of MMC in a binding site subject to extremely high energy barriers. However, rotamer libraries ignore the specific conformational effect of a particular protein environment. On the other hand, MC conformational search naturally takes the protein environment into account. Successful MC conformational studies on organic systems prompted the application of MC to proteins as well. MC strategy was applied for searching local interactions in the protein backbone by Rose et al. (*56*). Side chain conformations were predicted using low-temperature MC simulations by Shenkin et al. (*57*). Conformational studies on protein−substrate complexes were first performed by Guida et al. (*58, 59*) while comparative MC and MD docking calculations were published by our group (*5*).

The combined conformational search used in these docking calculations involves the variation of the internal degrees of freedom of the substrate and the binding site (rotatable bonds) as well as the external degrees of freedom of the ligand (relative translations and rotations) relative to the binding site. All of the internal and external degrees of freedom of the ligand and a limited set of internal degrees of freedom of the protein were considered. Results of our comparative MC/MD study presented on cytochrome P450 revealed that MC conformational analysis applied for proteins can be more effective than conventional MD simulations (*5*). Low-energy binding modes of NO in different electrostatic environments were therefore obtained using this new MC docking methodology.

Monte Carlo searches involved the random variation of all rotatable bonds combined with the so-called variable molecules selection (MOLS) for translations and rotations of the ligand in the binding site. The MOLS routine allows a selected molecule to move during a Monte Carlo step by randomly selected rotation and/or translation with respect to a fixed active site and, therefore, is particularly useful for docking calculations. The combined MCMM/MOLS procedure was applied to allow the simultaneous random translation and rotation of NO with respect to the active site with increments of 0.5−1.0 Å for the translation of the center of mass of the ligand along the *x*,*y*,*z* axes and, 30−180° for the rotation of the whole ligand around the *x*,*y*,*z* axes, respectively. This approach allowed us to look for all possible low energy binding modes of NO in a single MC simulation.

The initial random structures of the complex generated by the combined MCMM/MOLS procedure were subjected to restrained energy minimization applying a quadratic restoring potential to the backbone atoms of the active site. The constraint−substructure shell system described previously was used to keep the backbone atoms in the place where they are located in the crystal structure. The resulting minimum energy complex structures were sorted by energy, and the unique structures within a 50 kJ/mol energy window above the global minimum were stored in a MacroModel multistructure file for further interactive study using the three-dimensional graphical interface of MacroModel.

Conformational analysis of the enzyme−substrate complex involved 1000 Monte Carlo steps (MCMM/MOLS), and unique binding conformations were stored after rejections based on comparison of binding geometries of the substrate obtained in each step. Nonbonded atom pairs of extreme proximity give rise to very high van der Waals repulsion; therefore, trial structures having such close pairs were also discarded before minimization. Low-energy conformers obtained for the different orientations of His93 were analyzed by comparing the orientation of the substrate relative to the central heme unit. The number of duplicate structures obtained for each low-energy conformation was larger than 45, which proves our 1000 step MCMM search to be exhaustive. Since low-energy conformers were reproduced in a number of MCMM calculations using different starting geometries, this is also a clear indication of the completeness of the search.

The effectiveness of the MC approach was demonstrated in a comparative molecular dynamics simulation of NO in the same binding site model. Constant-temperature MD was performed at 300 K using the SHAKE algorithm (*60*) and the electrostatic treatment and constraint−substructure system described previously. The starting conformation was first

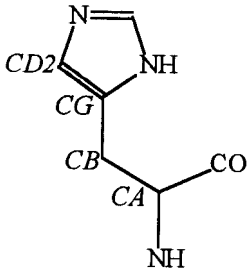

FIGURE 1: CA−CB−CG−CD2 torsion of His.

equilibrated for 30 ps before the accumulation of a 500 ps long dynamic data analysis. A total of 1000 structures were sampled periodically along equilibrated dynamic trajectories. These structures were finally subjected to energy minimization.

Electrostatic Calculations. Electrostatic interactions were calculated using the Delphi package (*61, 62*). The total free energy of solvation of NO by the protein was calculated as the sum of desolvation and interaction free energy terms. The desolvation energy equals half of the self-energy difference created by the transfer of the charged ligand from water to the uncharged protein. The interaction term was calculated as the product of the potential created by NO at the uncharged protein atomic sites and the corresponding atomic charges. Electrostatic charges were assigned to NO and the heme atoms including Fe (*35*); the rest of the protein carried Kollman-type charges, therefore, these latter values did not change with the changing conformation of His93. Calculations were focused in four steps to a final state where 90% of the calculation box was filled by the protein, the internal and external dielectric constants were set to 4 and 80, respectively, and the ionic strength was chosen to be 0.1.

RESULTS AND DISCUSSION

The electrostatic and conformational rearrangement of the MbFe(III)−NO complex as the function of the proximal histidine CA−CB−CG−CD2 torsion angle (Figure 1) was studied. Two different states of His93 were considered: one with a −113° torsional angle and another with a −125° torsional angle. The torsion of His93 is close to the −113° value in all myoglobin structures where the iron has six ligands, where NO, CO, O_2, or water is ligated to the heme; therefore, we called this value the ligand binding torsion of His93. However, studying crystal structures of distal side mutants of metmyoglobin (*63*) indicated that this residue might take up different conformations, too. In pentacoordinated structures of metmyoglobin where the ligand binding position is left empty (water binding site unoccupied) due to the steric or hydrophobic effect of mutated distal side residues, the described torsion of His93 tends to higher values, moving to −125°(see Table 1), which we called its ligand-free torsion. In previous work (*35*), we showed—using the proposed structure of the MbFe(III)−NO complex—that just by flipping His93, back-bonding between the ligand and Fe is weakened, the σ bonding between His93 and Fe is enhanced, and considerably rearranged electron density results for the heme and close-lying atoms.

Electrostatic Calculations. The torsional flip of His93 changes the atomic charge distribution both at the heme atoms and at NO (Figure 2). The dipole moment of NO decreases by approximately 10%; the charges of Fe and some heme atoms rearrange considerably too. To show, beside our conformational study, that these changes in electrostatics are characteristic Poisson−Boltzmann calculations using the program DelPhi (*61, 62*) were carried out to study the electrostatic interactions of NO with the rest of the protein as a function of the torsional flip of His93. The total solvation free energy of NO by the protein was calculated using charges corresponding to both torsions of His93. As can be seen in Table 2 the desolvation energy of NO by the protein is practically the same in both cases; however, specific interaction of the charges of NO with the rest of the protein is quite a bit more favorable (by 3.8 kJ/mol) when the torsion of His93 is at its ligand binding value; the overall effect is a 4.0 kJ/mol excess electrostatic stabilization of NO in this state. All protein segments with considerable contribution to the difference in interaction free energy of the two states are shown in Table 3. Of course the most important effect is the decrease of electrostatic attraction between the less positive charge of Fe and the practically unchanged charge of the N of NO at the −125° torsional value. The amino acids whose interaction with NO is most affected by the flip of His93 are the two histidines that keep the active region in place: the proximal His93 and the distal His64. Favorable interaction of NO with His64 is switched off at −125°; further modest destabilization from the interaction with His93 arises. The results demonstrate that the rearranged charges of the active site caused by the flip of His93 electrostatically destabilize NO in the close binding position, and therefore may contribute to the liberation of the ligand from Fe.

Table 1: Comparison of the Torsion Angle of His93 in Hexa- and Pentacoordinated MetMb Structures (SW = Sperm Whale, HH = Horse Heart)

name of PDB entry	mutation	water binding site (sixth coordination position)	torsion angle of His93 (deg)
pdb2mgj.ent[a]	His64Val	unoccupied	−124.7
pdb2mge.ent[a]	His64Leu	unoccupied	−122.0
pdb2mgi.ent[a]	His64Thr	partially occupied	−119.3
pdb2mgh.ent[a]	His64Gln	occupied	−113.5
pdb2mgb.ent[a]	His64Gly	occupied	−114.5
pdb4mbn.ent[b]	wild type, SW	occupied	−111.5
pdb1ymb.ent[c]	wild type, HH	occupied	−113.8

[a] Reference *63*. [b] Reference *67*. [c] Reference *68*.

Conformational Analysis Using the Charge Set Belonging to the Ligand Binding (−113°) Torsion of His93. The global minimum structure of the MD simulation of the complex contains the NO bound directly to the iron (see Figure 3). NO is bound in a bent conformation with the oxygen pointing toward the C pyrrole ring of the heme, making a 40.2° angle with the heme plane. The mean Fe−N distance was found to be 2.05 Å (see Figure 4). The crystal structure of the MbFe(III)−NO complex has not been determined yet, but the structure of MbFe(II)−NO is available (*64*). In this latter structure, the NO is bound 1.9 Å from the iron in a bent conformation also leaning toward the C pyrrole. The angle it creates with the heme is 24.50°. The structure derived by us is therefore in a quite similar arrangement to that measured for the MbFe(II)−NO complex, the main difference being that the NO is closer to linear binding in our calculations. Along the trajectory there was only one instance when the

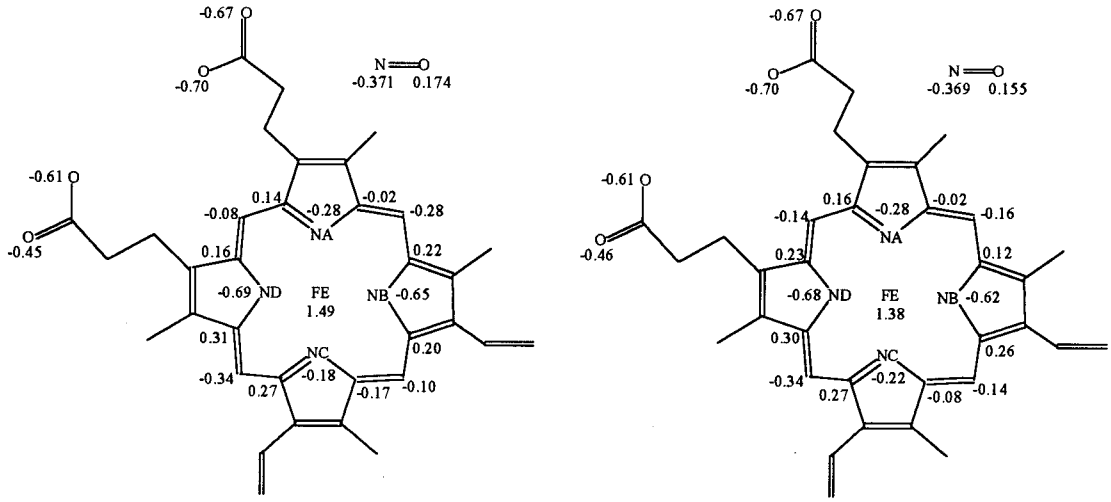

FIGURE 2: Some characteristic atomic charges of the ligand binding and ligand releasing charge set.

Table 2: Solvation Free Energy (ΔG_{Total}) of NO by the Protein as Calculated by DelPhi

	−113°	−125°
$\Delta G_{desolvation}$ (kJ/mol)	5.098	5.354
$\Delta G_{interaction}$ (kJ/mol)	−38.187	−34.412
ΔG_{total} (kJ/mol)	−33.089	−29.058

Table 3: $\Delta G_{interaction}$ Contribution of Different Protein Segments at the Two Different Torsions of His93

$\Delta G_{interaction}$ (kJ/mol)	−113°	−125°	$\Delta\Delta G_{interaction}$ [−113° − (−125°)]
Fe	−65.296	−62.301	−2.995
heme	26.827	26.970	−0.143
His64	−0.481	0.187	−0.668
His93	2.044	2.179	−0.135

NO escaped from the iron toward the hydrophobic interior of the protein, but it returned from this position immediately.

MC conformational analysis using the same charge set and the constraint−substructure system resulted in two conformations of the ligand, separated in relative energy by 12 kJ/mol. The more stable structure is identical with that found in the MD simulation (a1); in the conformer with excess energy, however, the NO is seen detached from the iron and inside a nearby hydrophobic pocket surrounded by Leu29, Leu32, Phe43, Val68, and Ile107 (h1).

Unconstrained MCMM/MOLS calculations afforded seven low-energy conformers. Six of these contained NO in the bound conformation with average Fe−N and Fe−O distances of 2.11 and 3.52 Å and an additional conformer with Fe−N and Fe−O distances of 4.08 and 5.40 Å corresponding to the a1 and h1 states, respectively.

It is interesting to see that the unconstrained MCMM/MOLS search provided the same results as the constrained one. Although, due to the greater mobility of the amino acid side chains, the number of low-energy conformers increased, the position and orientation of the NO molecule relative to the heme were simply the duplicate of the two different states derived previously.

Conformational Analysis Using the Charge Set Belonging to the Ligand Free (−125°) Torsion of His93. MD simulation resulted in one binding mode in this case as also seen in Figure 5; the NO was found inside the hydrophobic pocket

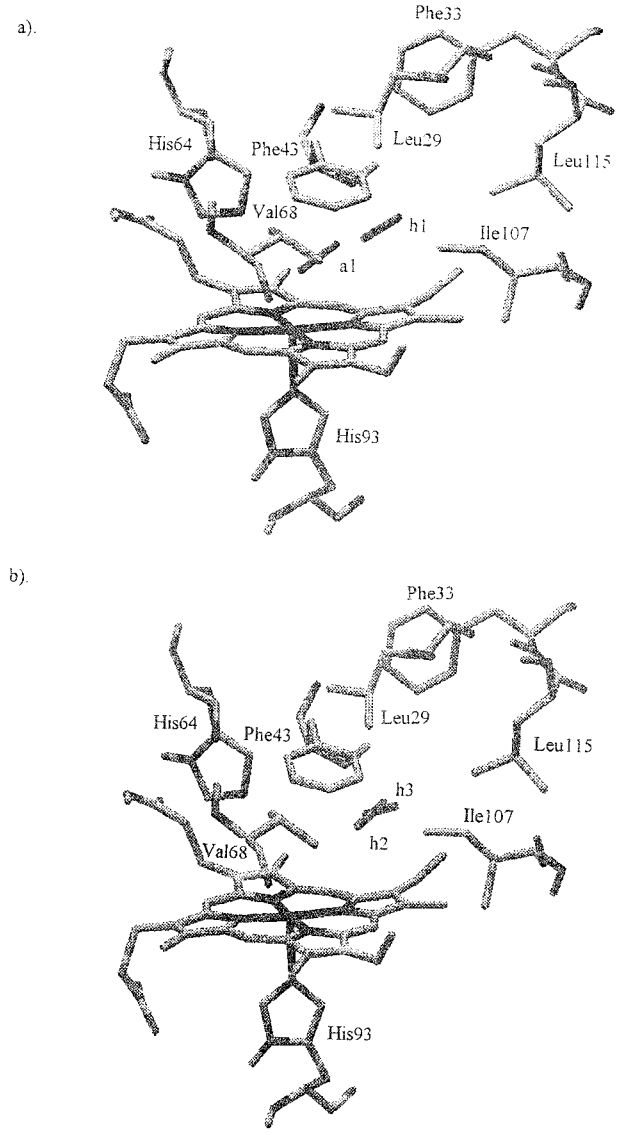

FIGURE 3: NO conformations obtained at the ligand binding (a) and ligand free (b) torsions of proximal His93 by MCMM/MOLS calculations.

created by Leu29, Leu32, Phe43, Val68, and Ile107 (h2). By the MCMM/MOLS method, two independent conformations (h2 and h3) were found, both within the same pocket,

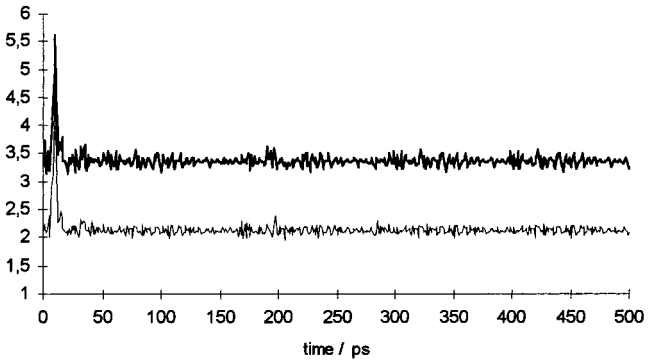

FIGURE 4: Fe−N (−) and Fe−O (**━**) distances in angstroms during MD simulation (GB/SA model applied) of the MbFe(III)−NO complex using the charge set belonging to the ligand binding torsion (−113°) of His93.

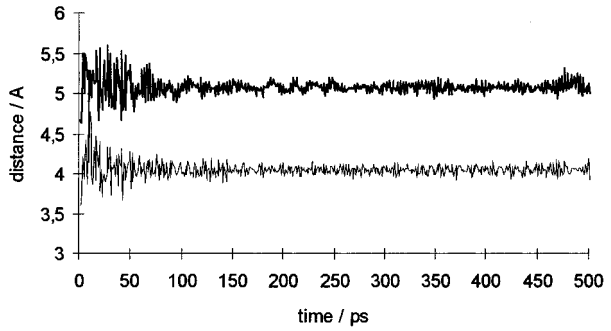

FIGURE 5: Fe−N (−) and Fe−O (**━**) distances in angstroms during MD simulation (GB/SA model applied) of the MbFe(III)−NO complex using the charge set belonging to the ligand free torsion (−125°) of His93.

Table 4: Distance from the Fe and Tilt of NO for All Determined Binding Conformations

	Fe−N distance (Å)	Fe−O distance (Å)	angle between heme plane and NO (deg)
a1	2.11	3.35	40.22
h1	4.07	5.24	21.64
h2	5.09	4.06	−21.85
h3	4.43	5.27	0.46

but with differing orientations, one of which is identical to that determined with MD. The energy of these two states is virtually identical.

Unconstrained MCMM/MOLS here also reproduced the results obtained for the constraint−substructure model system. Four of the seven low-energy conformers contained NO such that the N was closer to Fe (average Fe−N and Fe−O distances of 4.71 and 5.21 Å) while in three conformers the reversed orientation was found (Fe−N and Fe−O distances of 5.28 and 4.20 Å, respectively)—but in all cases, NO was within the described hydrophobic pocket.

Comparison of Conformations at −113° and −125°. Table 4 shows the Fe−N and Fe−O distances and the angle between the heme plane and NO for all four resultant conformations. h2 and h3 belong to the ligand-free torsion (−125°); a1 appears exclusively at −113°. This means that the charge rearrangement caused by the flip of His93 is indeed capable of destabilizing the NO ligand and prompts its dissociation from Fe. When the torsional angle of His93 is −113° (the ligand binding value), the NO associates to iron (a1), and its dissociation and geminate trapping are hindered by the high energy of the detached conformation

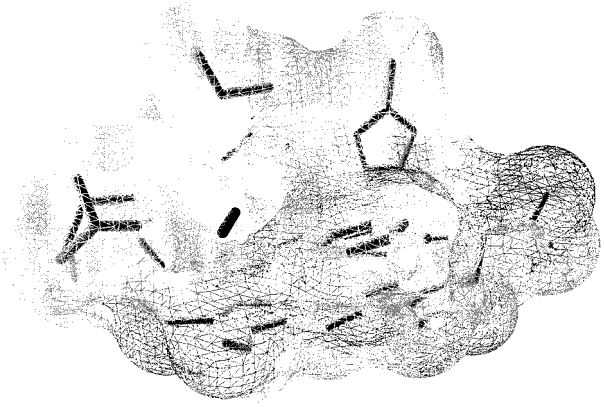

FIGURE 6: NO in binding position h2 inside the geminate hydrophobic pocket of MbFe(III) outlined by the van der Waals spheres of the surrounding amino acids. The surface was colored according to the potential generated by the protein; light gray indicates hydrophobic regions.

(h1). At −125°, however, no indication of close association to the iron can be found; instead, two energetically very similar geminately trapped conformations result (h2, h3). It is interesting to note that we did not see complete dissociation of the complex in either case; in other words, NO did not find its way out to the solvent, but was captured by the described hydrophobic pocket. Since h1 and h3 are quite similar to each other, h1 can actually be viewed as an intermediate between the bound (a1) and hydrophobic trapped (h3) conformations. The results thus suggest that three different binding modes of NO to metmyoglobin have to be considered: one associated with the iron (a1), and two in a geminate hydrophobic trap (h2 and h3). It should be noted that only two of these conformations could be derived with the MD method: a1 and h2.

The prompt response of NO seen upon switching to the nonbinding charge set is especially intriguing if we consider that the Coulomb attraction between Fe and NO is scaled back by less than 10% when flipping His93. The results demonstrate that quite subtle conformational or electrostatic changes can effectively disturb the heme−ligand interaction.

The hydrophobic cavity we found NO localized in (see Figure 6) as the result of nonbinding electrostatics is analogous with that determined as the geminate trap of CO in ferrous Mb by crystallography (*26*, *28*, *29*). CO was shown in femtosecond time-resolved IR measurements (*25*) to bind in this cavity in two opposing orientations; the energy difference of these two conformations was estimated to be about 1.2 kJ/mol. This result provides experimental support to our finding that NO can also flip within the hydrophobic docking site (conformers h2 and h3), as was shown by the MC analysis.

The direction of NO's initial movement after photodissociation was studied by Schaad et al. (*27*), who carried out MD simulation to explore the time frame of the NO geminate rebinding process. They simulated the effect of laser flash photolysis by switching between a nonbinding and a binding potential between six heme atoms and the atoms of the ligand. Using the nonbinding potential, NO did dissociate from the iron; however, a specific geminate trap was not localized,; only the most frequent collision sites were reported: Val68, Phe43, Ile107, Leu29, His64. These amino acids are, with the exception of His64, all part of the

geminate trap of CO, and that found by us for NO.

CONCLUSION

The position of NO within the active site of MbFe(III) was found to depend on the conformation of its proximal His93 residue. Different charge distributions corresponding to the two experimentally verified possible torsions of this proximal residue result in strong binding of the ligand or its release to the nearby hydrophobic trap. This supports our earlier proposition that the torsional flip of His93 is capable of selecting between ligand-bound and ligand-free states of metMb.

Three different conformations of bound NO have been determined: one associated with the iron (a1) seen when His93 is in its original conformation, and two different arrangements containing the NO in a nearby hydrophobic pocket (h2 and h3), the same cavity that was determined to be the geminate trap of CO in ferrous Mb, corresponding to His93 being flipped to its ligand-releasing orientation.

The release of NO from Fe upon the flip closely resembles the observed motion of CO upon photodissociation. Based on this, and our previously published analysis, we suggest that the conformational fluctuation of the proximal His results in the loosening and eventual break of the Fe−ligand bond and geminate trapping of the ligand. Conformational rearrangement of the proximal side would provide the possibility of rebinding of the ligand to Fe.

Both MD and MC methods were used to investigate the conformational space of the complex. MD, beside providing the global minimum structures for both charge distributions, was not able to locate higher energy, but still significant conformations. On the other hand, the MC algorithm applied located both global minima and other possibly populated conformations too, therefore proving more effective in mapping the relevant region of the potential surface.

ACKNOWLEDGMENT

We are grateful to É. Udvardy for pointing our interest to NO and I. Kolossváry for helpful discussions and carefully reading the manuscript.

APPENDIX

GB/SA continuum solvation model was developed for the approximate treatment of electrostatics in water by Still et al. (*65*). The generalized Born model (GB) applied here involves modeling of the electrostatic contribution of the hydration free energy by the Coulombic interaction in addition to a polarization term of the two-charge system:

$$\Delta G_{el} = \Delta G_{coul} + \Delta G_{pol} \quad (1)$$

Coulombic interactions are calculated by the formula:

$$\Delta G_{coul} = 166 \sum_{i \neq j} \frac{q_i q_j}{r_{ij}} \quad (2)$$

where q_i and q_j are the charges on atoms i and j, respectively, and r_{ij} is the distance between these atoms in units of kilocalories per mole. The polarization term is approximated by the eq 3:

$$\Delta G_{pol} = -166.0\left(1 - \frac{1}{\epsilon}\right)\sum_{i=1}^{n}\sum_{j=1}^{n} \frac{q_i q_j}{(r_{ij}^2 + \alpha_{ij}^2 e^{-D_{ij}})^{0.5}} \quad (3)$$

where $\alpha_{ij} = (\alpha_i \alpha_j)^{0.5}$ and $D_{ij} = r_{ij}^2/(2\alpha_{ij})^2$. α_i is the Born radius of atom i, and D_{ij} is the squared ratio of the i,jth atom pair separation of their mean Born diameter. Considering this mathematical formula, the Born radius of each atom having an atomic charge is required for the evaluation of the electrostatic free energy of solvation. α_i can be calculated by the equation:

$$\alpha_i = -\frac{166.0}{G'_{e,i}} \quad (4)$$

where G'_{ei} is the polarization energy of a hypothetical molecule in which all atoms but i are neutral. Although this solvation model avoids the repeated solution of the Poisson−Boltzmann equation, a fitting procedure is requested to determine the adjustable parameter in eq 3 so as to approximate the total hydration energy of two atoms in any molecule.

It is assumed that the neutral atoms displace the dielectric medium within their van der Waals surfaces, creating a solute-shaped cavity in the solvent-like medium. G'_{ei} can be calculated either numerically by summing the Born electrostatic energies of a series of concentric shells in the medium around the solute cavity (*65*), or analytically by assuming a unit charge on atom i and a surrounding medium of high dielectric ($1 - 1/\epsilon \sim 1$) (*13*). The analytical implementation of the GB model in MacroModel 6.0 is based on stretch, bend, and nonbonded interactions. This also means that long-range electrostatic polarization is taken into full consideration by the application of infinite electrostatic cutoffs.

The GB term discussed above is amended by another term proportional to the surface area (SA):

$$\Delta G_{cav} = \sigma \sum \alpha_i \quad (5)$$

where σ is a constant of proportionality independent of the atom type.

The cavity term (ΔG_{cav}) referred to as the free energy of cavity formation is added to the ΔG_{el} term to obtain the total contribution of the hydration effect. More details can be obtained from (*66*).

REFERENCES

1. Ajay, Mrucko, M. A., and Stouten, P. F. W. (1997) *Recent Advances in Prediciton of Binding Free Energies.* In *Practical Application of Computer-Aided Drug Design* (Charifson, P. S., Ed.) Marcel Dekker, New York.
2. van Gunsteren, W. F., and Mark, A. E. Q. (1992) *Eur. J. Biochem. 204*, 947.
3. van Gunsteren, W. F., King, P. M., and Mark, A. E. Q. (1994) *Rev. Biophys. 27*, 435.
4. Oda, K., Miyagawa, H., and Kitamura, K. (1996) *Mol. Simul. 16*, 167.
5. Keserű, G. M., Kolossváry, I., and Bertók, B. (1997) *J. Am. Chem. Soc. 119*, 5126.
6. Keserű, G. M., Kolossváry, I., and Székely, I. (1998) *Int. J. Quantum Chem.* (accepted for publication).
7. Jorgensen, W. L., and Nguyen, T. B. (1993) *Proc. Natl. Acad. Sci. U.S.A. 90*, 1194.
8. Duffy, E. M., and Jorgensen, W. L. (1994) *J. Am. Chem. Soc. 116*, 6337.

9. Jones-Hertzog, D. K., and Jorgensen, W. L. (1997) *J. Med. Chem. 40*, 1539.
10. Jorgensen, W. L., and Tirado-Rives, J. (1996) *J. Phys. Chem. 100*, 14508.
11. Essex, J. W., Severance, D. L., Tirado-Rives, J., and Jorgensen, W. L. (1997) *J. Phys. Chem. B 101*, 9663.
12. Jorgensen, W. L., and Ravimohan, C. J. (1985) *J. Phys. Chem. 83*, 3050.
13. Qiu, D., Shenkin, P., Hollinger, F. P., and Still, W. C. (1997) *J. Phys. Chem. A 101*, 3005.
14. Eich, R. F., Li, T., Lemon, D. D., Doherty D. H., Curry, S. R., Aitken, J. F., Mathews, A. J., Johnson, K. A., Smith, R. D., Phillips, G. N., Jr., and Olson, J. S. (1996) *Biochemistry 35*, 6976, and references cited therein.
15. Hoshino, M., Ozawa, K., Seki, H., and Ford, P. C. (1993) *J. Am. Chem. Soc. 115*, 9568.
16. Sharma, V. S., Isaacson, R. A., John, M. E., Waterman, M. R., and Chevien M. (1993) *Biochemistry 32*, 3897.
17. Gordunov, N. V., Osipov, A. N., Day, B. W., Zayas-Rivera, B., Kagan, V., and Elsayed, N. M. (1995) *Biochemistry 34*, 6689.
18. Griffith, O. W., and Stuehr, D. J. (1995) *Annu. Rev. Physiol. 57*, 707.
19. Ignarro, L. J., Buga, C. M., Wood, K. S., Byrns, R. W., and Chaudhuri, G. (1987) *Proc. Natl. Acad. Sci. U.S.A. 84*, 9265.
20. Palmer, R. M. J., Ferrige, A. G., and Moncada, S. (1987) *Nature 327*, 524.
21. Saavedra, J. M., Southan, G. J., Davies, K. M., Lundell, A., Hanson, S. R., Adrie, D., Hurford, W. E., Zapol, W. M., and Keefer, L. K. (1996) *J. Med. Chem. 39*, 4361.
22. Kagan, V. E., Day, E. W., Elsayed, N. M., and Gordunov, N. V. (1996) *Nature 383*, 30.
23. Petrich, J. W., Lambry, J.-C., Kuczera, K., Karplus, M., Poyart, C., and Martin, J.-L. (1991) *Biochemistry 30*, 3975.
24. Ansari, A., Dilorio, E. E., Dlott, D. D., Frauenfelder, H., Lnager, P., Roder, H., Sauke, T. B., and Shyamsunder, E. (1986) *Biochemistry 25*, 3139.
25. Lim, M., Jackson, T. A., and Anfinrud, P. A. (1997) *Nat. Struct. Biol. 4*, 209.
26. Hartmann, H., Zinser, S., Komninos, P., Schneider, R. T., Nienhaus, G. U., and Parak, R. (1996) *Proc. Natl. Acad. Sci. U.S.A. 93*, 7023.
27. Shaad, O., Zhou, H.-X., Szabo, A., Eaton, W. A., and Henry, E. R. (1993) *Proc. Natl. Acad. Sci. U.S.A. 90*, 9547.
28. Schlichting, I., Berendzen, J., Phillips, G. N. Jr., and Sweet, R. M. (1994) *Nature 371*, 808.
29. Teng, T. Y., Srajer, V., and Moffat, K. (1994) *Nat. Struct. Biol. 1*, 701.
30. Vitkup, D., Petsko, G. A., and Karplus, M. (1997) *Nat. Struct. Biol. 4*, 202.
31. Adachi, S., Nagano, S., Ishimori, K., Watanabe, Y., Morishima, I., Egawa, T., Kitagawa, T., and Makino, R. (1993) *Biochemistry 32*, 241.
32. Jewsbury, P., Yamamoto, S., Minato, T., Saito, M., and Kitegawa, T. (1994) *J. Am. Chem. Soc. 116*, 11568.
33. Rector, K. D., Rella, C. W., Hill, J. R., Kwok, A. S., Sligar, S. G., Chien, E. Y. T., Dlott, D. D., and Fayer, M. D. (1997) *J. Phys. Chem. 101*, 1468.
34. Rella, C. W., Rector, K., Kwok, A., Hill, J. R., Schwettmann, H. A., Dlott, D. D., and Fayer, M. D. (1996) *J. Phys. Chem. 100*, 15620.
35. Menyhárd, D. K., and Keserű, G. M. (1998) *J. Am. Chem. Soc. 120*, 7991.
36. Bernstein, F. C., Koetzle, T. F., Williams, G. J. B., Meyer, E. F., Jr., Bricem, M. D., Rodgers, J. R., Kenard, O., Shimanouchi, T., and Tasumi, M. (1977) *J. Mol. Biol. 112*, 535.
37. Nasri, H., Haller, K. J., Wang, Y., Huynh Boi Hahn, and Scheidt, W. R. (1992) *Inorg. Chem. 31*, 3459.
38. Obmolova, G. V., Safonova, T. N., Teplyakov, A. V., Popov, A. N., Kuranova, I. P., Arutyunyan, E. G., and Vainshtein, B. K. (1988) *Bioorg. Khim. 14*, 1509.
39. McDonald, D. Q., and Still, W. C. (1992) *Tetrahedron Lett. 33*, 7743.
40. Mohamadi, F., Richards, N. G. J., Guida, W. C., Liskamp, R., Lipton, M., Caufield, C., Chang, G., Hendrickson, T., and Still, W. C. (1990) *J. Comput. Chem. 11*, 440.
41. Whitlow, M., and Teeter, M. M. (1986) *J. Am. Chem. Soc. 108*, 7163.
42. Höltje, H. D., and Folkers, G. (1996) *Molecular Modeling: Basic Principles and Applications*, p 10, VCH, Weinheim, Germany.
43. Edinger, S. R., Cortis, C., Shenkin, P. S., and Friesner, R. A. (1997) *J. Phys. Chem. A 101*, 1190.
44. Honig, B., Sharp, K., and Yang, A.-S. (1993) *J. Phys. Chem. 97*, 1101, and references cited therein.
45. Marten, B., Kim, K., Cortis, C., Friesner, R. A., Murphy, R. B., Ringnalda, M. N., Sitkoff, D., and Honig, B. (1996) *J. Phys. Chem. 100*, 11775.
46. Scarsi, M., Apostolakis, J., and Caflisch, A. (1998) *J. Phys. Chem. B 102*, 3637.
47. Scarsi, M., Apostolakis, J., and Caflisch, A. (1997) *J. Phys. Chem. A 101*, 8098.
48. Straatsma, T. P., and McCammon, J. A. (1989) *J. Chem. Phys. 90*, 3300.
49. Straatsma, T. P., and McCammon, J. A. (1990) *J. Chem. Phys. 91*, 3631.
50. Wang, X., Erickson, S. D., Iimori, T., and Still, W. C. (1992) *J. Am. Chem. Soc. 114*, 4128.
51. Chang, G., Guida, W. C., and Still, W. C. (1989) *J. Am. Chem. Soc. 111*, 4379.
52. Goodman, J., and Still, W. C. (1991) *J. Comput. Chem. 12*, 1110.
53. Kolossváry, I., and Guida, W. C. (1996) *J. Am. Chem. Soc. 118*, 5011.
54. Senderowitz, H., Guarnieri, F., and Still, W. C. (1995) *J. Am. Chem. Soc. 117*, 8211, and references cited therein.
55. Li, Z., and Scheraga, H. A. (1987) *Proc. Natl. Acad. Sci. U.S.A. 84*, 6611.
56. Srinivasan, R., and Rose, G. D. (1995) *Proteins: Struct., Funct., Genet. 22*, 81.
57. Shenkin, P. S., Farid, H., and Fetrow, J. S. (1996) *Proteins: Struct., Funct., Genet. 26*, 323.
58. Guida, W. C., Bohacek, R. S., and Erion, M. D. (1992) *J. Comput. Chem. 13*, 214.
59. Montgomery, J. A., Niwas, S., Rose, J. D., Secrist, J. A., Babu, Y. S., Bugg, C. E., Erion, M. D., Guida, W. C., and Ealick, S. E. (1993) *J. Med. Chem. 36*, 55.
60. Ryckaert, J. P., Ciccotti, G., and Berendsen, H. J. C. (1977) *J. Comput. Phys. 23*, 327.
61. Sharp, K., and Honig, B. (1990) *Annu. Rev. Biophys. Chem. 19*, 301.
62. Sharp, K., and Honig, B. (1990) *J. Phys. Chem. 94*, 7684.
63. Quillin, M. L., Arduini, R. M., Olson, J. S., and Phillips, G. N., Jr. (1993) *J. Mol. Biol. 234*, 140.
64. Brucker, E. A., Olson J. S., Ikeida-Saito, M., and Phillips, G. N., Jr. (1998) *Proteins: Struct., Funct., Genet. 30*, 352.
65. Still, W. C., Tempczyk, A., Hawley, R. C., and Hendrickson, T. (1990) *J. Am. Chem. Soc. 112*, 6127
66. Keserű, G. M., and Kolossváry, I. (1999) *Molecular Mechanics and Conformational Analysis in Drug Design*, Blackwell Science, Oxford, U.K.
67. Takano, T. (1977) *J. Mol. Biol 110*, 537.
68. Evans, S. V., and Brayer, G. D. (1990) *J. Mol. Biol. 213*, 885.

BI981611V